PFC/JA–90–37

Research at MIT on High Frequency Gyrotrons for ECRH

Kreischer, K.E.; Grimm, T.L.; Guss, W.C.;
Temkin, R.J. and Xu, K.Y.

Plasma Fusion Center
Massachusetts Institute of Technology
Cambridge, MA 02139

October 1990

Submitted to Proceedings of Suzdal Meeting on Strong Microwaves in Plasmas
This work was supported by U.S. DOE Contract DE–FG02-89ER14052.

RESEARCH AT MIT ON HIGH FREQUENCY GYROTRONS FOR ECRH

K.E. Kreischer, T.L. Grimm, W.C. Guss,
R.J. Temkin, and K.Y. Xu

M.I.T. Plasma Fusion Center
Cambridge, MA., USA

Abstract

Research continues at MIT on high frequency (100-300 GHz) megawatt gyrotron oscillators suitable for ECR heating of fusion plasmas. Recent experiments include operation of a two-section cavity in the $TE_{16,2,1}$ mode at 148 GHz. Powers up to 1.2 MW were generated with a 78 kV, 48 A beam, yielding an efficiency of 32%. A peak efficiency of 39% was measured at 26 A. We are continuing our efforts to understand discrepancies between the measured and theoretical efficiencies at high current. Capacitive probes were installed to determine the average beam velocity ratio α. It was found that as the current increased, α corresponding to the highest output power decreased. At 35 A, the measured α was about 1.5, compared with a design value of 1.93. This reduction in α partially explains the discrepancy. We have also operated the gyrotron in a 14 T Bitter magnet into the submillimeter wave regime. Frequencies from 141 GHz ($TE_{15,2,1}$ mode) up to 328 GHz ($TE_{27,6,1}$ mode) were measured. Even though the cavity is highly overmoded at 328 GHz, output powers remain quite high, with a peak output power of 375 kW. Even better results were obtained in the $TE_{22,5,1}$ mode at 267 GHz, where a peak power of 537 kW was produced. The sequence of modes observed was consistent with the predicted coupling between the electron beam and rf field. Initial testing of a 1 MW, 280 GHz gyrotron is planned for early next year.

Introduction

Interest in ECR heating of fusion plasmas has grown in recent years. Advantages of ECRH include efficient, bulk heating of the plasma close to the magnetic axis, and the use of localized heating to modify the temperature profile and suppress plasma disruptions. ECRH can also be used in conjunction with an ion heating system, such as neutral beams, to produce a more balanced heating process and improve stability, or for current drive. From an engineering standpoint, ECRH sources can be located well away from the high radiation that exists near the plasma, and can utilize simple launching structures. Recent

experiments [1] indicate efficient ECR heating with local power deposition is possible, and that it is competitive with alternative heating techniques.

The main obstacle to ECRH has been the lack of suitable sources that can produce high power at the appropriate frequencies (100-300 GHz). However, the rapid development of novel, high power millimeter wave sources has mitigated this problem. In particular, extensive research over the past decade on the gyrotron has shown it to be a viable source for ECRH. The gyrotron is particularly attractive because it is very efficient, compact, and operates at low, cw voltages (< 100 kV). A large, international research effort has been established to study the gyrotron and determine its power and frequency capabilities. Powers up to 2.1 MW [2] and frequencies up to 328 GHz have been produced in ECRH-relevant experiments.

As gyrotrons operate at higher powers and frequencies, it becomes necessary to operate in higher order modes in order to maintain cavity ohmic losses at reasonable levels (below 2 kW/cm^2). Parametric studies [3] indicate that the index ν_{mp} of the lowest order $TE_{m,p,1}$ mode that can be utilized is given by the equation

$$(\nu_{mp}^2 - m^2) = \frac{2470\mu\beta_{\|}P(MW)\nu^{2.5}(GHz)}{\beta_{\perp}^2\rho_{ohm}(W/m^2)} \tag{1}$$

where $\mu = \pi\beta_{\perp}^2 L/\beta_{\|}\lambda$, $\beta_{\perp}$ and $\beta_{\|}$ are the perpendicular and parallel beam velocities normalized to c, ν and λ are the radiation frequency and wavelength, ρ_{ohm} is the average cavity ohmic losses, and L is the characteristic length of the axial rf field profile. Typically, $\mu \approx 15$, $\beta_{\perp} \approx 0.45$, and $\beta_{\|} \approx 0.25$. The cavity diameter D can be related to λ by the equation $D/\lambda = \nu_{mp}/\pi$. Early experiments were based on the $TE_{0,1,1}$ mode with $D/\lambda \approx 1$. Present experiments between 100 and 150 GHz have cavities with $D/\lambda \approx 5 - 10$, and the proposed MIT 1 MW, 280 GHz experiment will have a cavity with $D/\lambda \approx 20$. As D/λ increases, mode competition becomes more severe and high efficiency becomes harder to achieve.

The goal of the MIT program is to demonstrate new techniques for achieving efficient, single mode emission and improved output coupling in high frequency, megawatt gyrotrons. This includes the development of new diagnostics of gyrotron performance, thus allowing more rigorous comparison of experimental and theoretical results. We also are developing techniques for efficiently converting the high order modes of the gyrotron into a radiation beam that can be transmitted to a plasma. The long term goal of the M.I.T. program is to determine the highest powers that can be generated by high frequency gyrotrons suitable for ECRH. This research should provide the data needed to make a proper comparison between gyrotrons and alternative heating sources.

The MIT gyrotron operates at a low duty cycle ($\leq$4 Hz with 3μsec pulses). However, the cavity and electron gun are designed to be scalable to continuous (cw) operation. The magnetron injection gun was built by Varian and produces an annular beam with a theoretical $\beta_\perp/\beta_\parallel$ of 1.93 and a spread in $\beta_\perp$ of 4% at 80 kV and 35 A. The design magnetic compression is 30. The beam has a radius of 0.53 cm and thickness of 0.5 mm in the cavity region, and the current density when running at 35 A is 380 A/cm^2. The radiation produced is transmitted to the window by a copper waveguide with a typical diameter of 3 cm. The output window is either a single disk of fused quartz, or a broadband motheye window [4] with minimal reflection over a wide frequency range. The entire system is demountable for simple modification, and a gate valve between the gun and beam tunnel facilitates cavity changes. Two gyrotron test stands are presently available. The first uses a 6.5 T superconducting (SC) magnet with a six inch warm bore. The second has a 14 T Bitter magnet with a four inch bore, and allows us to generate frequencies up to 350 GHz. Both operate from a common, 20 MW pulsed power supply capable of 150 kV and a ripple less than $\pm$1%. Both also have a small gun coil for optimizing the beam quality.

Much of our experimental research has been based on the single, tapered cavity operating in asymmetric modes ($TE_{m,p,1}$ where $m \neq 0$). At the megawatt level, we have concentrated on operation in surface modes ($m \gg p$), which are situated close to the resonator wall. These modes provide good coupling between the rf field and electron beam, and reduced mode competition. Voltage depression due to the space charge field is also reduced. For our $TE_{15,2,1}$ experiments at 140 GHz, a depression of 3.3 kV was calculated for $R_e/R_o = 0.7$, where R_e and R_o are the beam and cavity radii. This corresponds to placement of the beam on the first radial maximum of the rf field. Potential problems with surface modes are the need for good alignment to avoid beam interception, and higher ohmic losses.

Efficiency Studies

A list of the theoretical and experimental characteristics of the cavities that we have investigated can be found in Table I. The best results in all three cases were achieved on the SC magnet test stand when operating in the $TE_{16,2,1}$ mode at 148 GHz. All the cavities were designed to operate near the minimum $Q = 4\pi(L/\lambda)^2$ in order to keep ohmic losses as small as possible. Self-consistent nonlinear theory [5] indicates efficiencies between 45% and 55% should be possible for these designs. The theoretical efficiency η_{TH} was calculated at 80 kV and 35 A, and was reduced by a total of 15% to account for an ohmic loss of 7% in the cavity, uptaper, and output waveguide, a calculated 5% dielectric loss in the output window, and other smaller losses. When operating at the maximum power P_{MAX}, we generally measured efficiencies between 22% and 32%. In all cases the best efficiencies η_{MAX} were obtained at lower currents, typically around 20-25 A.

Table I. Theoretical and measured characteristics of the MIT gyrotron

	Short	Long	Two–Section
L/λ	4.8	6.0	6.3
Q	311	468	508
I_{ST} (A)	4.2	1.8	1.5
P_{TH} (MW)	1.26	1.40	1.46
η_{TH} (%)	45	50	52
P_{MAX} (MW)	0.93	0.77	1.2
η (%)	22	26	32
V (kV)	104	84	78
I (A)	40	36	48
η_{MAX} (%)	30	34	39

This reduction in efficiency at higher currents is highlighted in Fig. 1. This figure shows results from our first experiments, which used the long cavity. The voltage was fixed at 70 kV, and the magnetic fields at the cavity and gun were optimized. We found that the measured efficiency saturated at low current, and remained relatively constant (between 25% and 35%) over a broad range of currents (5A to 30A). Two theory curves are shown, one based on an $\alpha = \beta_\perp/\beta_\parallel$ of 1.93, and the other on beam velocities as measured by our capacitive probe [6]. Both theory curves indicate that the efficiency should peak at 30-35 A, in contrast to our observations of a peak at lower currents. Our capacitive probe indicates that α decreases from 2.0 at 5A to 1.55 at 35A. This reduction is consistent with our experimental observation that, for fixed beam voltages, it is necessary to raise the gun magnetic field at higher beam currents, and therefore reduce the magnetic compression, in order to achieve high power, stable operation and avoid arcing in the electron gun. Figure 1 indicates that a reduction in α partially explains the lower efficiencies at higher currents.

Various attempts were made to increase the output power beyond the 770 kW generated at 84kV and 36A. These included operating in $TE_{m,2,1}$ modes other than the $TE_{16,2,1}$, tuning the cathode power supply to produce a flatter pulse, using windows of different thicknesses, and running at higher beam voltages and currents. In all cases the improvement was minimal. Tapering of the magnetic field in the cavity was also investigated. Tapering becomes more difficult at higher frequencies because of the higher magnetic fields required and the need to taper over a shorter axial distance. In our case, a modest taper of $\pm 1.5\%$ was possible. Both positive and negative tapers were tried with the $TE_{16,2,1}$

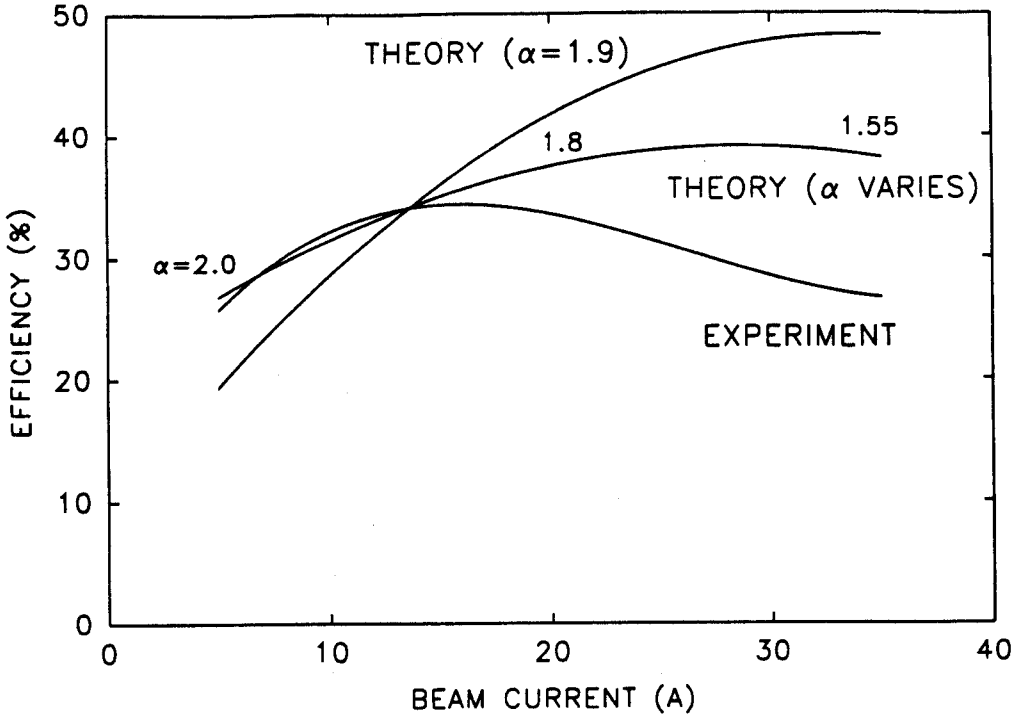

FIG. 1 Comparison of theory and experiment for the long cavity

mode, and in both cases the efficiency dropped about 10% compared to the uniform field results. One possible explanation is deleterious effects on the gun performance when the SC magnetic field is tapered. When the taper is introduced, it is not localized to the cavity region, and the entire axial field profile is modified. Finally, a new cavity with a shorter interaction length was designed and tested. It was hoped that by reducing the cavity Q that the higher efficiencies would shift to higher current. Also, this cavity has a higher starting current I_{ST} of 4.2 A. Multimode theories [7] suggested that mode competition might become a problem if the ratio of the operating current to I_{ST} becomes too large. However, this cavity produced lower efficiencies than the long cavity, probably due to the shorter L (see Table I).

The two-section cavity was selected for our next experiment. This cavity consists of two cylindrical sections of slightly different radii, followed by a linear uptaper. The two cylindrical sections produce an rf axial field profile with a long tail at the cavity input. This tail is known to slightly perturb the beam, causing the electrons to form a tighter bunch that enhances the final efficiency [8]. Simulations confirm these results (see Table I.). This cavity also produces higher efficiencies than our previous cavities for α less than 1.9. For example, when α is 1.5, the two-section cavity can achieve 45% compared to 33-41% for the long and short cavities. The diameters of the two sections are only slightly different, and virtually no mode conversion is produced. Ohmic losses are comparable to

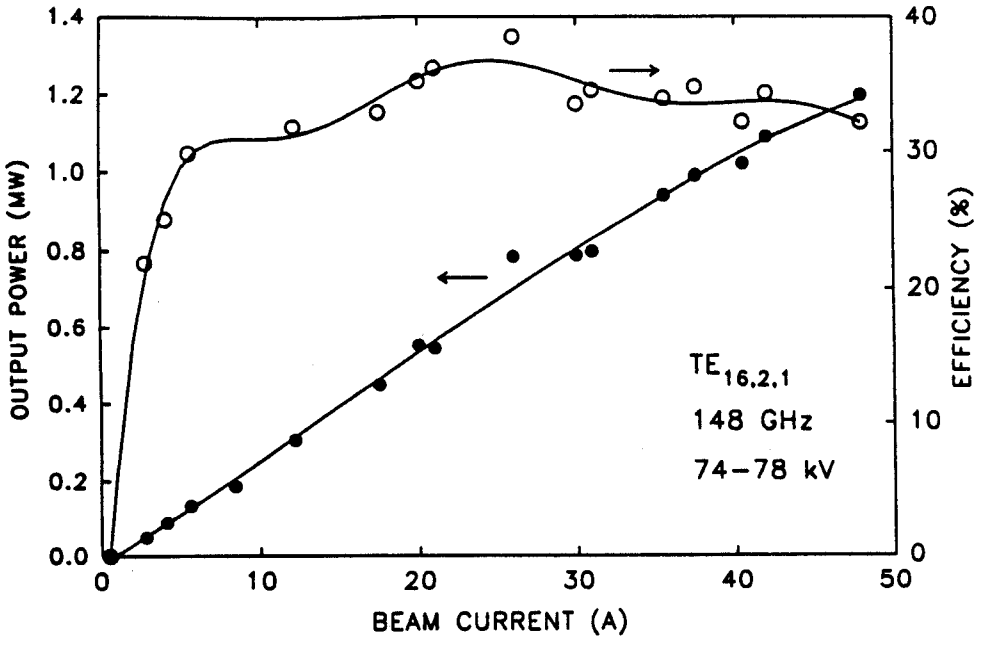

FIG. 2 Experimental results for the two-section cavity.

the other cavity designs.

The input cylindrical section of the two-section cavity was made relatively long to prevent rf leakage back towards the gun. Also, no input taper was included. It was hoped elimination of this taper would prevent higher order axial modes from becoming trapped in the cavity. However, calculation of the cold cavity properties indicated that the second axial mode could exist with a Q of about 600, comparable to the desired mode. Fortunately, simulations with the beam present indicated that this mode should be weak, and that the first axial mode should dominate. It was also hoped that removal of the input taper would reduce competition with transverse modes. This would happen because the frequency of such a mode would increase by about ω/Q due to pulling, and would therefore not be cutoff at the cavity input. This would increase leakage for this mode and lower its Q.

The results of our experiments are shown in Figs. 2-4. In Fig. 2, the maximum emission as a funtion of beam current is shown. For each setting, the magnetic fields at the cavity and gun were optimized. In all cases, single mode emission was observed in the $TE_{16,2,1}$ with a frequency of about 148 GHz. A maximum power of 1.2 MW was obtained at 48 A, for an efficiency of 32%. As in our earlier studies, the efficiency rises quickly as the current is increased, and remains relatively constant between 30% and 40%. A maximum of 39% was measured at 26 A. A comparison between theory and experiment is shown in Fig. 3. The α values shown were obtained with our probe, and again they decrease as the

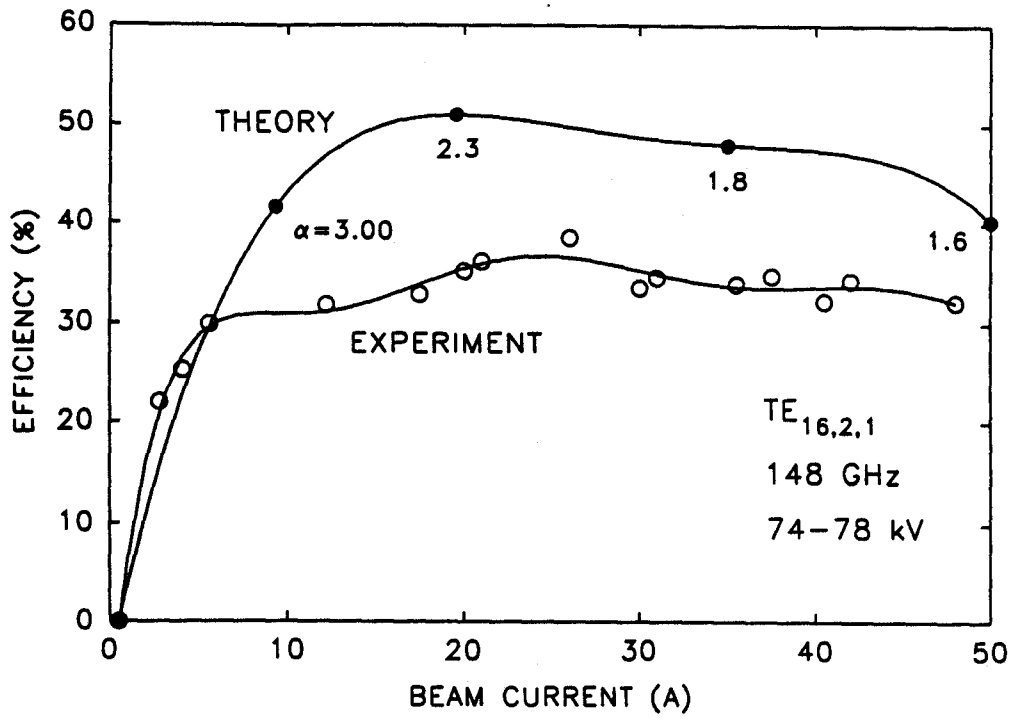

FIG. 3 Comparison of two-section cavity results with theory.

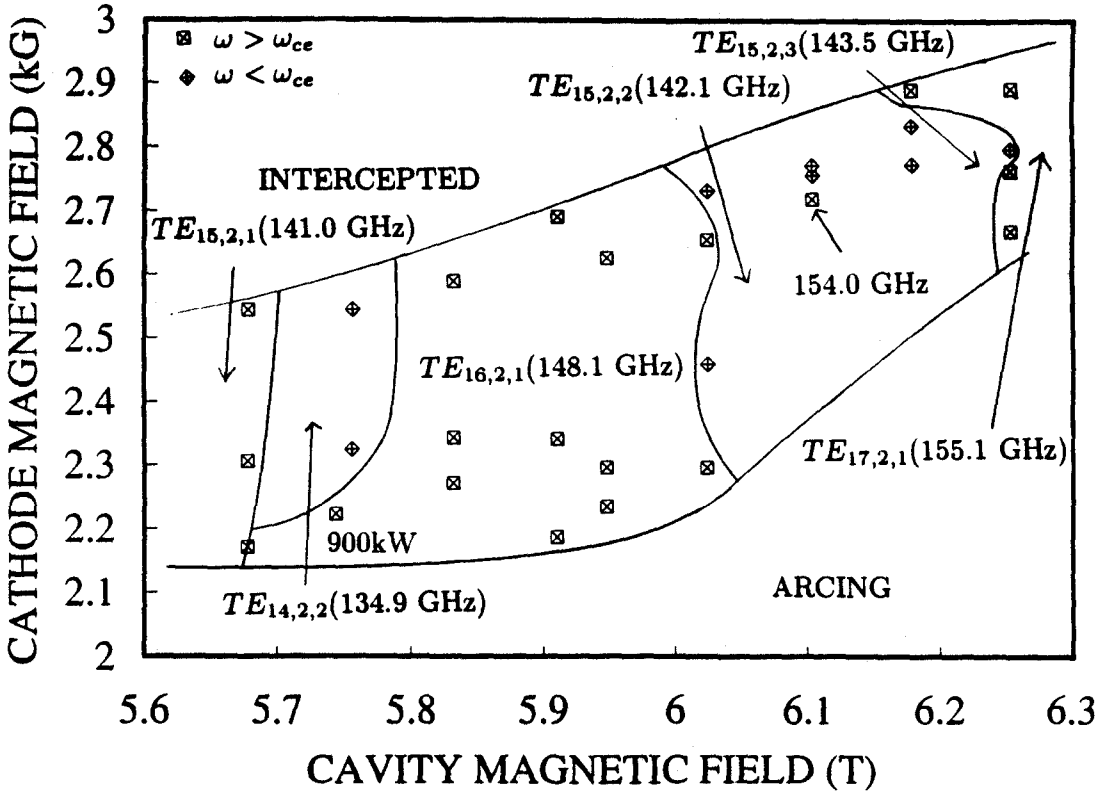

FIG. 4 Mode map for 74 kV, 35 A operation.

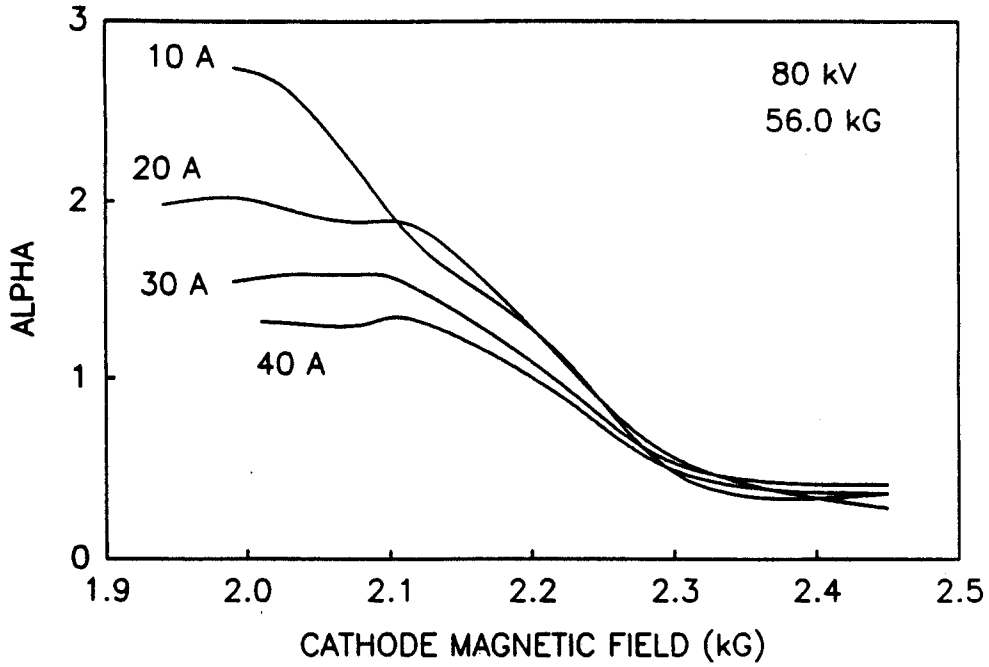

FIG. 5 Measured average α for 1 MW, 140 GHz gun.

beam current increases. Although the discrepancy continues to exist between theory and experiment, it is smaller for this cavity. Also, the variation in α seems to be responsible for the saturation of the efficiency. A detailed mode map is given in Fig. 4 for operation at 74 kV and 35 A. Only the cathode and cavity magnetic fields were varied to generate the data. As the cathode field is increased, the beam expands leading to interception before the cavity. If this field is too small, some of the electrons are mirrored, resulting in an arc. This is consistent with adiabatic theory. The dominant modes are the $TE_{m,2,1}$, which are separated by weaker regions of $TE_{m,2,2}$. The frequencies are in good agreement with theoretical values. No emission was observed in the $TE_{m,3,1}$ modes, which were the main competing modes in the long and short cavity. Based on a comparison of ω and ω_c, it was found that the backward branch of the $TE_{m,2,2}$ modes was being excited. Theory indicates [9] that this branch is more accessible than the forward branch. Access to the forward branch is blocked by the stronger $TE_{m,2,1}$ modes during startup of the gyrotron. The highest power of 900 kW occurs at low cathode magnetic fields where α is the highest. The detuning parameter $\Delta = 2/\beta_\perp^2(1 - \omega_c/\omega\gamma)$ for this operating point is 0.56, consistent with theory.

In addition to the study of novel cavities, we are also developing diagnostics to measure the beam spatial and velocity characteristics. We have impacted the beam on a tantalum foil to produce images. Our concern was that instabilities, such as the diocotron instability, could be causing filamentation of the beam. The images indicated that the beam

density is uniform, and measurements of the diameter and thickness agree with theoretical predictions. To measure the average velocity properties, a capacitive probe was installed in the beam tunnel just before the cavity. This probe consists of two concentric cylinders that measure the static radial electric field of the nonneutral beam. which is then related to the beam density. From this and the current, an average parallel velocity is determined which in turn gives the average α. The capacitive probe works as a passive diagnostic and allows the power and α to be measured simultaneously. No effect on gyrotron performance has been seen.

Probe measurements have shown that α generally agrees with adiabatic theory in its scaling versus cathode magnetic field and anode voltage. An example is shown in Fig 5, which shows how the MW gun operates in the Bitter magnet. At large cathode magnetic fields, α is small as expected. As the field is reduced, α increases and then saturates. The saturation level is dependent on the beam current, and decreases as the current increases. For a 35 A beam, the maximum α measured was between 1.4 and 1.6, well below the design value of 1.93. At present the explanation for this saturation is not known.

We are also developing diagnostics to measure the velocity spread. Theory indicates that perpendicular spreads in excess of 10% are needed before the efficiency is substantially reduced. Two approaches that we have investigated are a retarding potential [10], and measurement of the starting current. In the first approach, a slotted plate selects a small portion of the beam, which is then collected by a plate biased by a repelling voltage. The change in the collected current as this voltage is varied gives the $\beta_{\|}$ electron distribution function. This diagnostic must be carefully designed to minimize the effects of secondary emission and reflected electrons. Measurement of the starting current does not directly measure the distribution function, but can give an indication of the amount of spread present. A short cavity was designed with a starting current of 35 A when α is 2. When a parallel spread of 30% is present (assuming a Gaussian distribution), the current is reduced to 18 A. Tests with this cavity are now in progress.

Submillimeter Operation

We have observed fundamental, submillimeter emission by operating up to 13 T with a Bitter magnet. These experiments were based on the long cavity described in Table I. The diffractive Q ranges from 460 at 140 GHz to 2300 at 328 GHz. A sequence of $TE_{m,p,1}$ modes with p=3 through 6 was excited by varying the cavity magnetic field B_o. This step tunability is shown in Fig. 6. Changing B_o causes a series of discrete modes to be excited in the cavity. For each mode in Fig. 6, the cathode magnetic field B_k was adjusted to

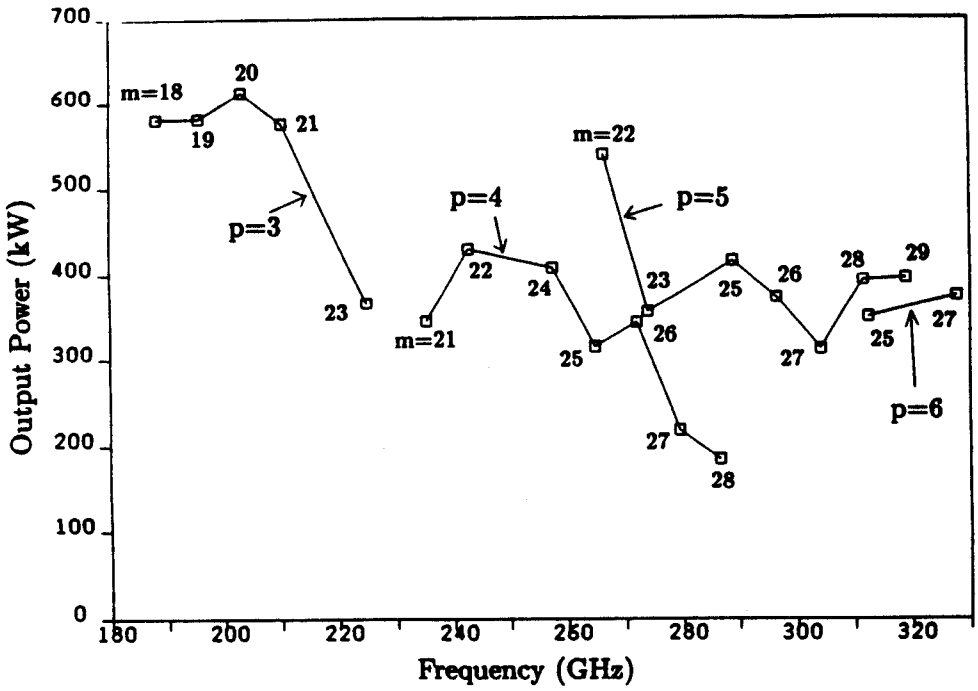

FIG. 6 Step tuning through a sequence of $TE_{m,p,1}$ modes with an 80 kV, 35 A beam.

maximize the output power. Output power was measured outside a fused quartz output window. Window losses are about 2% at 180 GHz and increase to greater than 13% at 330 GHz. Although the electron gun design was optimized for operation at 140 GHz, this data indicates that a high quality beam is produced over a wide range of frequencies. The power levels are generally between 300 and 600 kW, and depend on the coupling strength between the beam and rf field, as well as the beam α.

The sequence of modes observed is consistent with the radial position of the beam within the cavity. Nonlinear theory indicates that the coupling between the beam and rf field scales as $J_{m\pm1}(2\pi R_e/\lambda)$, where R_e is the beam radius and the choice of sign depends on the azimuthal rotation of the mode. The strongest coupling occurs when the beam interacts with the first maximum of $J_{m\pm1}$, that is, when $2\pi R_e/\lambda \approx \nu_{m\pm1,1}$. For modes with $m >> 1$, this expression can be written as $2\pi R_e/\lambda \approx m \pm 1$. As B_o is increased, resulting in operation at shorter λ, R_e decreases slightly due to higher magnetic compression B_o/B_k, but the λ scaling dominates. Therefore higher m modes are excited at higher frequencies, as is observed. The radial index p is determined by the relative position of the beam and cavity wall. The cavity radius R_o was chosen such that the beam would couple to the first radial maximum of the $TE_{15,2,1}$ mode at 140 GHz. This also results in strong coupling to neighboring $TE_{m,2,1}$ modes when B_o is varied. As B_o is increased, higher magnetic compression is required to produce a high α beam necessary for strong

emission. This causes the beam to move away from the wall, and eventually the beam decouples from the $p = 2$ modes and couples to the first radial maximum of the $p = 3$ modes. This process continues until the strongest coupling at 328 GHz is to the $p = 6$ modes.

The results at 328 GHz ($TE_{27,6,1}$) represent the highest powers generated by a gyrotron in the submillimeter region. For an 80 kV, 15 A beam the output power and efficiency of the $TE_{27,6,1}$ mode was 214 kW and 18% respectively. At 35 A the power increased to 375 kW for an efficiency of 13%. This corresponds to 430 kW and an efficiency of 15% when window losses are excluded. Although the cavity is highly overmoded at 328 GHz, with a cavity diamter of 16.4λ, the power remains quite high. This suggests that mode competition has not strongly limited the operation of the gyrotron and prevented access to the high efficiency regime. The major problem, especially in pulsed experiments, is exciting the desired mode first so that it can suppress neighboring competing modes.

Even better results were obtained in the $TE_{22,5,1}$ mode at 267 GHz. The output power and efficiency for this mode as measured after the window is shown in Fig. 3. Window losses are about 9%. At each beam current the emission was maximized by varying B_k. The mode was excited by beam currents up to 45 A with a maximum efficiency of 27% and power of 330 kW at 15 A. This power increased to 537 kW at 35 A for an efficiency of 19%. As in our 140-150 GHz measurements, the highest efficiencies occurred at lower currents.We also found that the $TE_{22,5,1}$ mode could be excited over a wide range of parameters, again suggesting that mode competition was not a major limiting factor.

280 GHz Experiments

The next major U.S. tokamak project is C.I.T., an ignition device with a nominal magnetic field of 10 T. This experiment will need 0.5-1 MW gyrotrons operating between 250 and 300 GHz. Although we have already achieved similar parameters, the cavity used was too small to be cw relevant (i.e., ohmic losses were too high). Equation (1) indicates that operation in a very high order $TE_{m,p,1}$ mode, with $(\nu_{mp}^2 - m^2)^{0.5} > 60$ is required. A list of the parameters of the first experiment can be found in Table II, together with the present 140 GHz parameters. The major constraints on the 280 GHz design were the cavity ohmic losses (limited to an average of 2 kW/cm^2), the anode-cathode electric field in the gun (kept below 80 kV/cm to avoid breakdown) and the gun radius smaller than the magnet bore radius. The last constraint allows the gyrotron tube to be assembled and baked outside the magnet, as is presently done with industrial tubes. The cost of the magnet scales strongly with bore size, so there is a strong incentive to keep the bore diameter small. Table II indicates many 280 GHz parameters are similar to parameters of our present experiment, giving us confidence that the experiment will be successful. The

Table II. 1 MW Design Parameters

	140 GHz	280 GHz
Current(A)	35	37
Voltage(kV)	80	90
$\eta_T(\%)$	36	30
Velocity ratio	1.93	1.6
Beam radius(cm)	0.53	0.75
Cavity radius(cm)	0.75	1.25
Cavity length(L/λ)	6.0	7.0
Diffractive Q	450	620
Magnetic compression	30	44
Cavity current density(A/cm^2)	384	660
Beam thickness(r_L)	3.85	4.2
Voltage depression(%)	4.0	5.6
Emitter radius(cm)	2.89	4.9
Mode	$TE_{15,2,1}$	$TE_{42,7,1}$
Mode separation(GHz)	7.2	4.5

major changes are the radial dimensions of the cavity and beam, and the need to operate in a very high order mode. For our experiments the beam has been postioned on the first radial peak for maximum coupling.

The two major components are a 12 T SC magnet and 1 MW electron gun. The magnet is being built by Wang NMR and contains both NbTi and Nb_3Sn coils. Specifications include a five inch warm bore, field dropoff to 0.3 T at the gun emitter, low helium losses, quench protection, and an optional linear taper of 4%/inch. The main parameters of the gun were calculated using adiabatic theory. Using the highest anode-cathode electric field consistent with cw operation (80 kV/cm), a gun with a magnetic compression of 44 was designed. This gun has an emitter radius of 4.95 cm, and will operate at 90 kV and 50 A. The Herrmannsfeldt gun code was used to optimize the electrode shapes. A design was found with a perpendicular velocity spread of $\pm 5.0\%$. Initial operation of this experiment is expected in the first half of 1991.

Acknowledgements

This research is supported by the Department of Energy under Contract DE-AC02-78ET51013. The Bitter magnet was provided by the Francis Bitter National Magnet Laboratory. The authors wish to thank M. Basten, M. Blank, W. Mulligan and G. Yarworth for their assistance in the experiments.

References

[1] R. Prater *et al.* in *Plasma Physics and Controlled Fusion*, 1988, Proceedings Twelfth International Conference, Nice (IAEA, Vienna, in press).

[2] A. Sh. Fix *et al.*, Int. J. Electron. **57**, 821 (1984).

[3] K.E. Kreischer, B.G. Danly, J.B. Schutkeker, and R.J. Temkin, IEEE Trans. Plasma Science **PS-13**, 364 (1985).

[4] J.Y.L. Ma and L.C. Robinson, Opt. Acta **30**, 1685 (1983).

[5] A. Fliflet, M. Read, K. Chu, and R. Seeley, Int. J. Electron. **53**, 505 (1982).

[6] W.C. Guss, T.L. Grimm, K.E. Kreischer, J.T. Polevoy, and R.J. Temkin, MIT report PFC/JA-90-13, submitted to J. Appl. Phys. (1990).

[7] O. Dumbrajs, G. Nusinovich, and A. Pavelyev, Int. J. Electron. **64**, 137 (1988).

[8] Yu. V. Bykov, A. L. Goldenberg, Radiophys. Quantum Electronics **18**, 1066 (1975).

[9] K.E. Kreischer and R.J. Temkin, Int. J. Infrared Millimeter Waves, **2**, 175 (1981).

[10] E.G. Avdoshin and A. L. Goldenberg, Radiophys. Quantum Electronics **16**, 461 (1973).